

Computational microscopy in embryo imaging

Joseph L. Hollmann*

Department of Electrical and Computer Engineering, Northeastern University, Boston, Massachusetts 02115

Andrew K. Dunn

Massachusetts General Hospital, Nuclear Magnetic Resonance Center, Harvard Medical School, Building 149, 13th Street, Charlestown, Massachusetts 02129

Charles A. DiMarzio

Department of Electrical and Computer Engineering, 440 Dana Building, Northeastern University, Boston, Massachusetts 02115

Received May 5, 2004

The growth of computing power has greatly improved our ability to extract quantitative information about complicated three-dimensional structures from microscope images. New hardware techniques are also being developed to provide suitable images for these tasks. However, a need exists for synthetic data to test these new developments. The work reported here was motivated by studies of embryo health, but similar needs exist across the field of microscopy. We report a rigorous computer model, based on Maxwell's equations, that can produce the required synthetic images for bright-field, differential interference contrast, interferometric imaging, and polarimetric imaging. After a description of the algorithm, sample results are presented, followed by a discussion of future plans and applications. © 2004 Optical Society of America

OCIS codes: 180.0180, 180.3170, 180.6900.

A new computational model for microscopy is reported. The motivation for this work arose during the development of a new interferometric microscope for imaging embryos to determine their viability. We have developed a new instrument, the quadrature tomographic microscope,¹ that is similar to the Jamin–Lebedeff interferometric microscope,² except that it uses a polarization technique for detecting both phases of an optical field.³ It provides an alternative to other means of determining the phase of an optical field, such as the use of multiple intensity measurements.⁴

These two-dimensional images are not simple slices of a three-dimensional image. To a first approximation, they are integrals of the index of refraction along a ray propagating from source to receiver, suggesting reconstruction methods inspired by x-ray computed tomography scans. The next level of complexity accounts for diffraction and suggests reconstruction with diffraction tomography.⁵ This is still a simplification resting on the assumptions of the first Born approximation, and the structure of the embryo violates these assumptions.

These reconstruction processes both involve precise rotation of the specimen on the microscope stage, which is a difficult task. A simpler approach to three-dimensional imaging is Z stacking: focusing the microscope in small increments to different depths through the object. As every microscopist is aware, it is possible to discern some three-dimensional structure by moving the focus knob on the microscope. Nevertheless, we know that the optical transfer function in three dimensions is a toroid with a null at the origin, and this limits our ability to recover three-dimensional information. Techniques using structured lighting can avoid this null but still offer limited resolution in the axial direction.⁶ With noise present, full three-dimensional reconstruction will never be perfectly accurate, but, because we are asking for a relatively

small amount of information, statistical aggregation characteristics of mitochondria and a simple count of the number of cells, these simpler measurements may well suffice. To determine whether this is true, we need to examine Z stacks of known objects, and the best way to do this with certainty is to use synthetic data. Because of the high density of mitochondria and the relatively large size of cells compared with the wavelength, we cannot rely with certainty on the first Born or Rytov approximation to provide a suitable forward model for generating these data.

This Letter reports on the generation of synthetic Z stacks by using an existing finite-difference time-domain (FDTD) computer model to compute the field in the pupil and a Fresnel–Kirchhoff integral to compute the field in each image plane.

Figure 1 illustrates the method. In the FDTD model a plane wave is propagated through a computational space that contains our object of interest, as shown in the upper left panel of the figure. The resulting field at the boundaries is propagated to

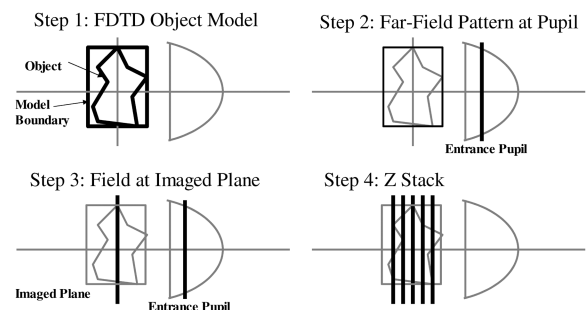


Fig. 1. (a) Method of computation begins with the FDTD computation to obtain the field throughout the volume. (b) Next the complex field is computed in the pupil plane and (c) propagated to the image plane. (d) The latter two steps are repeated for each image plane.

the far field where we place the pupil of the lens of the microscope (upper right). This is accomplished by weighting the FDTD results with a three-dimensional Green's function and integrating over the volume.⁷

We can employ the Fresnel–Kirchhoff integral to propagate the field to the imaged plane (lower left panel in the figure):

$$U(x, y, z) = \frac{2ik \exp[ik(z - z_1)]}{4\pi(z - z_1)} \exp\left[ik \frac{x^2 + y^2}{2(z - z_1)} \right] \times \iint_{\text{aperture}} U_A(x_1, y_1, z_1) \exp\left[ik \frac{x_1^2 + y_1^2}{2(z - z_1)} \right] \times \exp\left[\frac{ikxx_1}{(z - z_1)} \right] \exp\left[\frac{iky y_1}{(z - z_1)} \right] dx_1 dy_1.$$

Here the desired field as a function of x and y in an image plane at depth z is $U(x, y, z)$. The field in the pupil is $U_A(x_1, y_1, z_1)$, k is the scalar wave number, and the integral is over the aperture at the pupil. Quite simply, the formula adds a slight curvature to the field, uses the two-dimensional Fourier transform to propagate the field through space, and then flattens it out again.

This allows us to simulate focusing the microscope to different depths (lower right panel in figure) above and below the object center. It is important to note that finding the refocused field is not the same as finding the original field at that depth plane.

We developed a series of tests to validate the three-dimensional FDTD program and generate progressively more complicated simulated images. Our first test simulated a field propagating through a transparent glass bead with a diameter of $20 \mu\text{m}$ and an index of reflection of 1.5 in water with an index of reflection of 1.33. By propagating the field back to image plane $z = 0$, we see in Fig. 2 that the simulated results are consistent with measurements. The left panel of the figure shows the simulation, and the right panel shows real data with a somewhat larger bead. The simulation is currently limited, on our computers, to a volume with dimensions of a cube slightly larger than $20 \mu\text{m}$, whereas available beads are somewhat larger. In both cases the phase was unwrapped with a two-dimensional phase-unwrapping routine.⁸

After refocusing the field in small increments to positions along its depth axis, we generated a plot in the $x-z$ plane, with the amplitude shown in Fig. 3. As expected, the bead focused its transmitted field into a severe bright spot in the forward direction, as is observed in experimental images.

With this result for a simple geometry as a test case, we moved on to a more complicated geometry. Our next test simulated a large sphere in water with an index of 1.33 encapsulating three smaller, equisized spheres, as shown in the line drawing in Fig. 4. The three small spheres had an index of refraction of 1.37, whereas the larger sphere had an index of refraction of 1.35. The result of focusing the field to the $z = 0$ plane at the center of the larger sphere yields little information alone. By focusing the field to the centers of each of the smaller beads, we are able to ascertain

their presence as shown in the images in Fig. 4. The overall pattern is much more complicated than that of the single sphere, but the individual components of the object are each visible at appropriate image planes. In the future we wish to test our ability to decode the geometry and optical properties of the object through analysis of the three-dimensional images.

The next test case uses a cell with a few mitochondria carefully positioned to determine our ability to locate and resolve them in three dimensions. One mitochondrion is located at the center of the cell at the

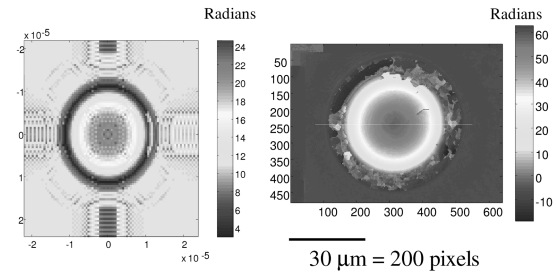


Fig. 2. Images of the phase of an image of the simulation and experimental data for a glass sphere in water.

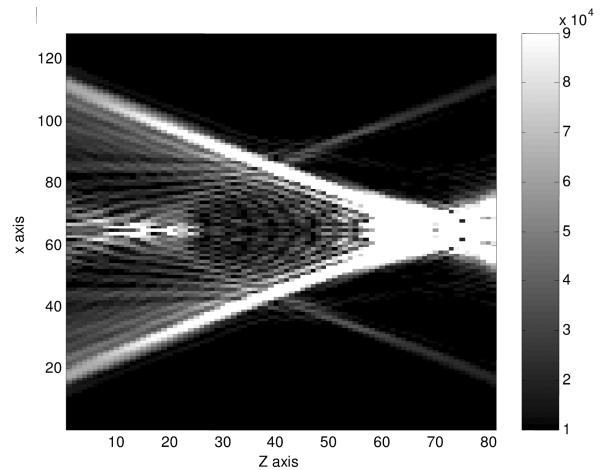


Fig. 3. Same image as shown in Fig. 2, as a function of x and z , for $y = 0$. Note the focusing effect.

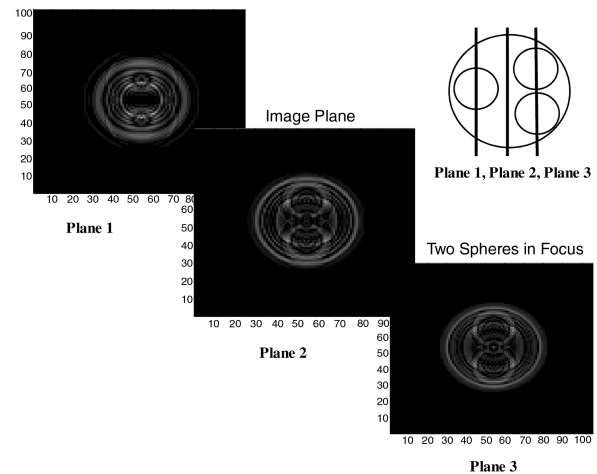


Fig. 4. Three spheres inside a larger sphere. Indices of refraction for the background, large sphere, and all three smaller spheres are 1.33, 1.35, and 1.37, respectively.

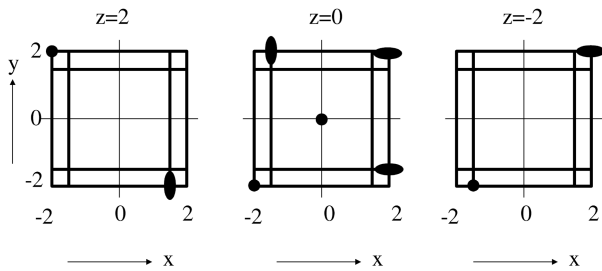


Fig. 5. Arrangement of mitochondria for a test case. The mitochondria are ellipsoids distributed in three planes to test our ability to locate and resolve their locations.

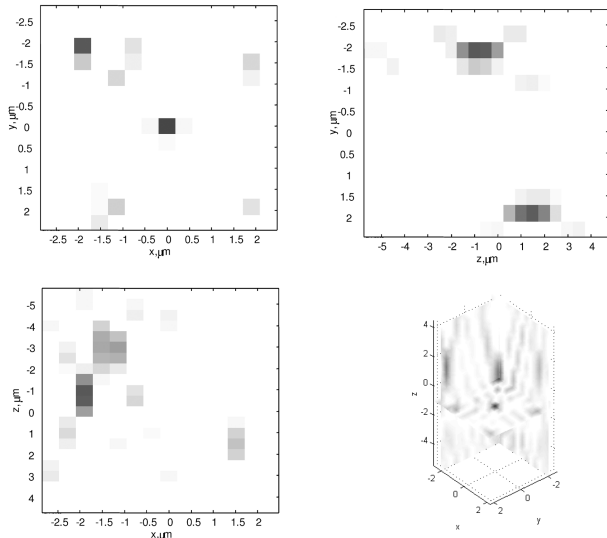


Fig. 6. Images of a sphere with objects inside it as shown in Fig. 5. The upper left panel shows the amplitude as a function of x and y for z at $1 \mu\text{m}$ below focus. The lower left panel shows an x, z plot for $y = -3 \mu\text{m}$. The upper right panel shows a y, z plot for $x = -3 \mu\text{m}$. The lower right panel shows some slices in a three-dimensional view.

origin of the x, y, z coordinate system. Four more are located in the $z = 0$ plane, and two each are located in the $z = -2$ and $z = 2$ planes, as shown in Fig. 5. The mitochondria are modeled as ellipsoids with diameters of $0.5 \mu\text{m}$ in two of the principal directions and $1.5 \mu\text{m}$ in the third. Sample images are shown in Fig. 6. Only a small central volume, $5 \mu\text{m}^2$ in x and y and $10 \mu\text{m}$ deep in z , is reconstructed, so the outer boundary of the sphere is not visible in these pictures. Each of the mitochondria is observed, located, and resolved. Because of diffraction effects, some artifacts begin to appear, which will complicate the picture as more mitochondria are introduced.

This Letter has illustrated the ability of our model to generate realistic synthetic quantitative Z stack data, allowing us to evaluate a microscope's ability to locate and resolve features in a three-dimensional object. For sufficiently simple objects with sufficient

contrast and high spatial frequencies, such as a few mitochondria, the model confirms the well-known fact that the objects can be located directly from the Z stacks. For large objects, such as the cells themselves, some type of reconstruction algorithm will be required. The synthetic data provide a method for validating such algorithms. Likewise, for a cell with more than 100,000 mitochondria, the complicated interactions of all the scattered fields will require at least some image processing to determine useful properties of their distribution, and the synthetic data will be critical to understanding the requirements and evaluating the resulting algorithm.

The present model runs on a cluster of four Pentium 3 machines at 1 GHz and requires 6–12 h, with a total memory requirement of 2–4 Gbytes. With the help of advances in parallel computing we need to increase the size of the model to approximately $100 \mu\text{m}^3$. We may also need to compute the pupil field on a more dense grid to allow for higher numerical apertures and fields of view.

Additional applications include variations in the input field, for structured-lighting or confocal microscopy. Different states of polarization are handled correctly on both input and output. In conclusion, this model provides a rigorous method for generating synthetic data for a variety of microscopic imaging techniques.

Portions of this work were funded by the Center for Subsurface Sensing and Imaging Systems under the Engineering Research Centers Program of the National Science Foundation (award EEC-9986821) and by a grant to A. Dunn from the Whitaker Foundation. C. A. DiMarzio's e-mail address is dimarzio@ece.neu.edu.

*Current affiliation, Texas A&M University, College Station, Texas 77843.

References

1. C. A. DiMarzio, A. J. Devaney, and S. C. Lindberg, "Optical quadrature interferometry utilizing polarizing optics," U.S. patent 5,883,717 (March 16, 1999).
2. M. Slayter and H. S. Slayter, *Light and Electron Microscopy* (Cambridge U. Press, Cambridge, England, 1992).
3. D. O. Hogenboom, C. A. DiMarzio, T. J. Gaudette, A. J. Devaney, and S. C. Lindberg, *Opt. Lett.* **23**, 783 (1998).
4. Noniterative Reconstruction of Complex Valued Objects from Two Intensity Measurements. With M. H. Maleki and A. J. Devaney *Opt. Eng.* **33**, 3243 (1994).
5. A. J. Devaney, *Ultrason. Imaging* **4**, 336 (1982).
6. M. G. L. Gustafsson, D. A. Agard, and J. W. Sedat, *J. Microsc.* **195**, 10 (1999).
7. A. Dunn and R. Richards-Kortum, *IEEE J. Sel. Top. Quantum Electron.* **2**, 898 (1996).
8. D. Ghiglia and M. Pritt, *Two-Dimensional Phase Unwrapping: Theory, Algorithms, and Software* (Wiley, New York, 1998).